



Biosorptive removal of basic dye methylene blue using raw and CaCl₂ treated biomass of green microalga *Scenedesmus obliquus*

Hany H. Abdel Ghafar^{a,b}, Mohamed A. Embaby^{a,c}, Emad K. Radwan^{b,*},
Azza M. Abdel-Aty^b

^aDepartment of Chemistry, Faculty of Sciences and Arts, Khulais, University of Jeddah, Saudi Arabia,
emails: hany_ghafar@hotmail.com (H.H. Abdel Ghafar), embaby_mn@yahoo.com (M.A. Embaby)

^bDepartment of Water Pollution Research, National Research Centre, 33 El Bohouth St., Dokki, Giza, Egypt 12622,

Tel. +202 33370931; Fax: +202 33371211; emails: emadk80@gmail.com (E.K. Radwan), azzamy@hotmail.com (A.M. Abdel-Aty)

^cDepartment of Food Toxicology and Contaminants, National Research Centre, 33 El Bohouth St., Dokki, Giza, Egypt 12622

Received 19 January 2017; Accepted 2 July 2017

ABSTRACT

Dyes can cause significant problems to the aquatic environment and food chain, therefore, their removal is one of the main concerns. This study was performed to explore the potential of *Scenedesmus obliquus* to remove dyes from aquatic environment. A series of batch biosorption experiments were done to evaluate the effect of contact time, solution pH and biomass dosage on the sorption process. The pseudo-first-order and pseudo-second-order kinetic models were applied to study the biosorption kinetics. The equilibrium data were analyzed by Freundlich, Langmuir and Dubinin–Radushkevich. The Fourier transform infrared spectroscopic results highlighted the importance of the functional groups on the biomass cell wall in the sorption process. The sorption results revealed that more than 70% of the dye was removed in 10 min. Also, the biosorption process was strongly dependent on the biomass dosage with an optimum removal at 1.2 g/L. The pseudo-second-order model gives the best fit to the kinetic data and suggests that the adsorption rate of the raw biomass is six times that of the treated one. Freundlich model was found to be the best fit to the equilibrium data. It suggests higher uptake capability of raw biomass compared with the CaCl₂ treated one. The methylene blue (MB) uptake by the biomasses was a chemisorption process as indicated by the pseudo-second-order kinetic, Freundlich and Dubinin–Radushkevich models. This study proved that *S. obliquus* can efficiently remove MB from aqueous medium and the treatment of *S. obliquus* with CaCl₂ has detrimental effect on its sorption capacity.

Keywords: Biosorption; Isotherms modeling; Adsorption kinetics; Green algae; River Nile; Pre-treatment

1. Introduction

Dyes are widely used in textiles, leather, paper, plastics, rubber, cosmetics, pharmaceutical and food industries [1]. Dyes are toxic to microorganisms and harmful to human health [2–4]. It has been reported that dyes cause carcinogenesis, teratogenicity, mutagenesis and respiratory toxicity [5]. The discharge of dyes into water resources even in low concentrations can cause many significant problems to

the aquatic environment and food chain. They deplete the oxygen content and reduce sunlight penetration which affect photosynthetic activities leading to disturbance of the aquatic equilibrium [6]. Therefore, the removal of dyes from contaminated water has been considered as main concern to minimize the environmental and toxicology threats posed to human and aquatic environment and to preserve the water resources [7].

Various physical, chemical and biological methods have been used for the treatment of dye containing wastewater. Biosorption is a physicochemical process that utilizes low cost materials such as live or dead biomass to remove

* Corresponding author.

contaminants and deals with the sorption of a chemical substance in/on a biological surface [8]. Different types of biosorbents such as bacteria, algae, fungi and plant have been investigated for their ability to sequester dyes and other organic pollutants [9–12].

Recently, biosorption employing algae to remove dyes from the polluted waters has been proposed [13–15]. Algae are highly effective, reliable and economic in the removal of dyes from aqueous solutions. Several algal species such as *Gracilaria corticata* [16], *Sargassum muticum* [17], *Ulva lactuca* [18], *Gelidium* [19], *Enteromorpha* spp. [20], *Cystoseira barbatula* Kützinger [21], and *Nizamuddinina zanardinii*, *Gracilaria parvispora* and *Ulva fasciata* [22] have been investigated as biosorbents for methylene blue (MB). In the recent years, research has been focusing on increasing the sorption capacity of algal biomass through the chemical and physical pre-treatments [22,23]. However, no specific trend can be drawn, in other words, the pre-treatments can either increase or decrease the adsorption capacity [24].

In this context, this work reports for the first time the ability of the raw and chemically treated dead cells of freshwater green alga *Scenedesmus obliquus* to remove MB from aqueous medium. Also, the effect of contact time, pH, and biomass dosage on the biosorption process was studied. Additionally, the equilibrium data of the biosorption studies were modeled using different isotherm models. Finally, the pseudo-first-order and pseudo-second-order kinetic models were studied to investigate the sorption behavior.

2. Materials and methods

2.1. Chemicals

MB was selected as a model substrate in this study. Table 1 represents the chemical structure and selected properties of MB. Working solutions of MB were prepared from a stock solution of 1 g/L by dilution to give the desired initial concentration for each experiment. All solutions were prepared using deionized water and all reagents were of analytical grade and were provided by Merck (Darmstadt, Germany).

2.2. Biomasses preparation

The biomass used in this study was prepared from a freshwater green alga *S. obliquus*, which was isolated from phytoplankton community of the River Nile, purified and recultivated in a fresh algal nutrient medium BG11 [25]. The

cultures were kept at $24^{\circ}\text{C} \pm 2^{\circ}\text{C}$ under continuous illumination of fluorescent lamps with intensity of $33.8 \mu\text{E}/\text{m}^2/\text{s}$. No aeration was provided. The cultures were hand shaken daily to prevent cell clumping and adherence to the flasks. At maximum growth, the algal cultures were harvested by centrifugation at 5,000 rpm for 10 min. They were thoroughly washed with distilled water several times to remove residual nutrient. The washed biomass was then dried in an oven at 40°C (to a constant weight), then crushed, milled and sieved into fractions. The particles of 0.2 mm size fraction were selected for biosorption experiments. The raw *S. obliquus* biomass was denoted as RSO hereafter and was stored in an airtight bottle until use.

2.3. Biomass pre-treatment

The biomass was modified using 0.2 M CaCl_2 solution, herein, a known quantity (5 g) of dry *S. obliquus* biomass (0.2 mm) was suspended in 250 mL of 0.2 M CaCl_2 solution for 24 h under slow stirring. The solution was kept at constant pH 4 (optimum pH value for calcium activation). Treated *S. obliquus*, denoted as TSO hereafter, was separated from the mixture by filtration. The collected sample was washed with distilled water to remove the excess calcium, oven dried at 40°C to constant weight, crushed and sieved through a 0.2 mm sieve.

2.4. Characterization of biosorbents

In order to recognize any probable interaction between the biomasses surface functional groups and MB, the powder of RSO and TSO before and after MB biosorption was examined using Fourier transform infrared spectroscopy (FTIR). The samples were dried and grounded with KBr and the mixture was pressed to produce pellets and analyzed using “Jasco FT/IR-6100A” within the range of $400\text{--}4,000 \text{ cm}^{-1}$.

2.5. Biosorption experiments

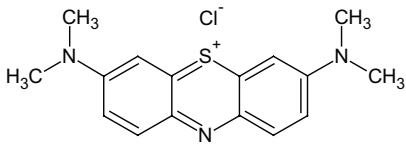
Batch biosorption experiments were performed at room temperature ($25^{\circ}\text{C} \pm 0.1^{\circ}\text{C}$) by adding the biosorbent to a series of aqueous solutions exactly contain 100 mL of MB solution of known concentration in a 250 mL stopper conical flasks. The flasks were shaken by a mechanical shaker (Drawell SK-L180-Pro) at 120 rpm. Samples were withdrawn, filtered and the residual MB concentrations in the filtrate were measured using a UV-Vis spectrophotometer (Shimadzu UV-2600) at the wavelength of 664 nm.

The removal percentage ($R \%$) and biosorption capacity, the amount of MB sorbed per gram of algal biomass at equilibrium (q_e , mg/g), were calculated according to Eqs. (1) and (2), respectively, by measuring the concentration of MB before and after biosorption process.

$$R\% = \left(1 - \left(\frac{C_e}{C_i} \right) \right) 100 \quad (1)$$

$$q_e = (C_i - C_e) \frac{V}{m} \quad (2)$$

Table 1
Selected properties of MB

| | |
|------------------------|---|
| Chemical structure |  |
| Molecular formula | $\text{C}_{16}\text{H}_{18}\text{ClN}_3\text{S}$ |
| Molar mass | 373.90 g/mol |
| Chromophore | Azo-dye |
| λ_{max} | 664 (nm) |

where C_i and C_e are the initial and equilibrium MB concentration in the solution (mg/L), respectively, V is the MB solution volume (L) and m is the biosorbent weight (g).

For each series of measurements, duplicate samples were analyzed and mean of the results were used in calculations, a procedural blank was run under similar experimental conditions but in the absence of sorbent and did not show a significant loss of MB on the container walls. A standard was analyzed routinely with each batch of samples. Also, all the UV–Vis was calibrated regularly and calibration was verified before each sample set.

2.5.1. Biomass amount effect

To determine the effects of biomass dose on MB removal efficiency, the biosorbent dose was varied from 0.20 to 1.40 g/L. The MB solutions (natural solution pH is 6.5) were kept under shaking for 1 h then samples were filtered, and the filtrate was analyzed for residual MB concentrations.

2.5.2. pH effect

In order to determine the effects of pH on MB removal efficiency, biosorption was studied at pH 3–9. In each of the experiments 100 mL of 20 mg/L MB solution was adjusted to the appropriate value with 0.1 M NaOH or HCl solutions. The pH was measured by a digital pH meter (GOnDO PL-700PV). After the pH adjustment, the solutions were mixed with 0.12 g of biosorbent then the procedure was continued as described above.

2.5.3. Kinetics study

To investigate the biosorption kinetics, batch experiments were performed as described above. In brief, 0.1 g of the biosorbent was added to 100 mL of 20 mg/L MB (natural solution pH is 6.5) and the flasks were shaken for 80 min. Samples were withdrawn at a predetermined time intervals, filtered, and the filtrate was analyzed for residual MB concentrations. The pseudo-first-order and pseudo-second-order kinetic models were applied to study the biosorption kinetics.

2.5.4. Isotherms study

In order to illustrate the biosorption isotherms, the batch procedure described above was used at the optimum conditions (1.2 g/L biosorbent and pH 5). Initial MB concentration was varied within the range of 10–100 mg/L. To describe the mechanism of MB biosorption on the studied biomass, the Langmuir, Freundlich and Dubinin–Radushkevich (D–R) isotherm models were tested.

3. Results and discussion

3.1. Characterization of the biomass

Fig. 1 shows the various functional groups on the cell wall of the RSO, MB loaded RSO (denoted as MB-RSO), TSO and MB loaded TSO (denoted as MB-TSO). Qualitatively, all the studied biomasses show similar IR spectra. Yet, careful analysis of the spectra can disclose differences in features. The broad band at $3,427\text{ cm}^{-1}$ might be a result of the

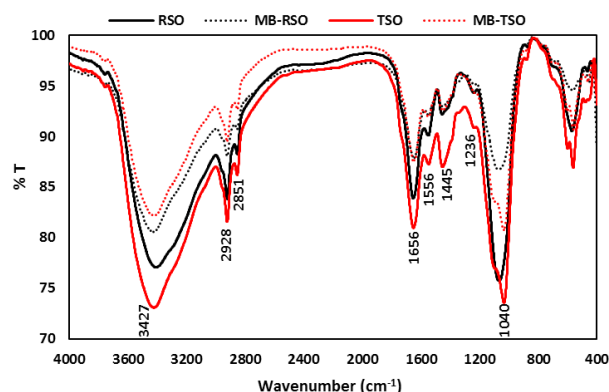


Fig. 1. FTIR spectra of raw, modified and MB loaded *Scenedesmus obliquus*.

overlapping of O–H and N–H stretching vibrations, suggesting the existence of both surface hydroxy stretching of carboxylic groups and stretching of amido groups. Other peaks around $2,928/2,851\text{ cm}^{-1}$ and $1,656\text{ cm}^{-1}$ can be attributed to the methylene C–H asymmetric/symmetric stretching and alkenyl C=C stretching, respectively. The band at $1,556\text{ cm}^{-1}$ represents the N–H bending and indicates the presence of secondary amine. The peak at $1,445\text{ cm}^{-1}$ could be assigned to methyl C–H asymmetric bending. The bands at $1,236\text{ cm}^{-1}$ were assigned to the aromatic ethers, aryl–O stretching. The band observed at $1,040\text{ cm}^{-1}$ is due to the alkyl substituted ether, C–O stretching. Therefore, FTIR analysis evident the existence of several functional groups on the cell wall of the RSO and TSO which might be generated by their complex polysaccharides, protein and lipid components [20].

Generally, pre-treatment has a trivial effect on the bands intensities and wavenumbers. Contrarily, the bands intensities have been significantly decreased after loading both RSO and TSO with MB. This indicates that the surface functional groups of the biomasses might play an important role in the biosorption process. Similar results have been reported previously [26]. Furthermore, the decrease in the bands intensities for the MB loaded biomasses was very similar for both RSO and TSO suggesting that the pre-treatment has negligible effect on the adsorption characteristics of the biomasses.

3.2. Optimum conditions

3.2.1. Effect of biomass amount

The variations of the removal percentage of MB as a function of the biomass dose are shown in Fig. 2. The results show that the MB removal percentage increases as the biomass dose increased up to 1.2 g/L then hardly changed. Such a trend is typically ascribed to increasing the sorptive surface area and the availability of more active sorption sites with increasing the biomass dose.

In addition, Fig. 2 shows that the extent of increase in the removal percentage with the biomass dose was relatively greater in case of TSO. Furthermore, TSO achieve higher removal percentage at the optimum biomass dose. It has been reported that the aggregates are formed at high adsorbent dose. Aggregation formation reduces the total surface area and increase the diffusional path length consequently

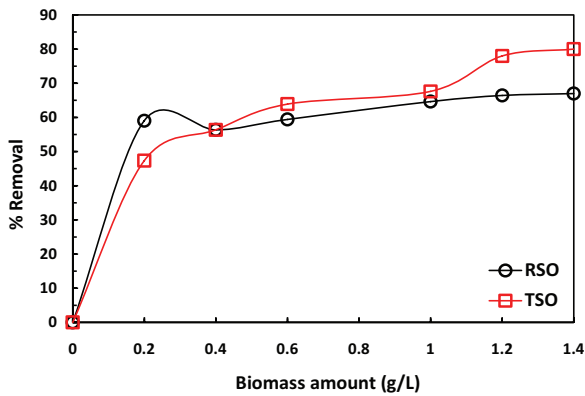


Fig. 2. Effect of biomass dose on the removal of MB. Experimental conditions: contact time, 40 min; C_i 20 mg/L and pH, 6.5.

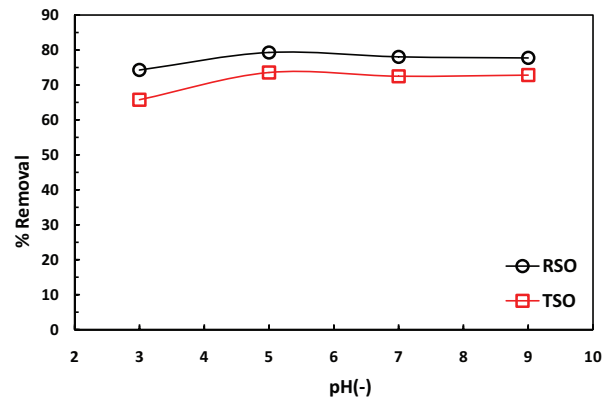


Fig. 3. Effect of pH on the removal of MB. Experimental conditions: contact time, 40 min; C_i 20 mg/L and dose, 1.2 g/L.

decrease the biosorption capacity [27]. It seems that the chemical treatment decreases the aggregation tendency of the biomass accordingly improve the biosorption capacity. This behavior is in accordance with the literature [20,21]. Therefore, the sorbent dosage in subsequent experiments was selected as 1.2 g/L.

3.2.2. Effect of pH

Fig. 3 presents the relationship between the initial solution pH and the removal percentage of MB by the studied biomasses. As shown, for both RSO and TSO, the removal percentage was increased by increasing pH from 3 to 5 and remained almost constant thereafter. However, the change in the removal percentage as a function of pH was negligible in case of RSO while for TSO the removal percentage was 66 at pH 3 then increased to 73 at pH 5 and remains nearly constant afterward. Moreover, the pre-treatment of the RSO has a slight detrimental effect on its sorption efficiency.

As mentioned in the discussion of FTIR results, the cell wall of the studied biomasses contains a number of charged functional groups such as carboxyl and hydroxyl groups. Hence, at lower pH, the hydronium ions compete the cationic dye toward active sorption sites resulting in a decline in the removal percentage. At higher pH the algal cell wall may get neutral or even negatively charged, which enhances the biosorption of the cationic dye through electrostatic forces of attraction. Similar trend have been reported for the biosorption of MB by other biomasses [18,20,21,28].

3.3. Effect of contact time and kinetics study

Equilibrium time is a very important factor in the design of cost-effective treatment systems. Fig. 4 (a) shows the change of the percentage removal of MB with time vs. the initial MB concentration. It can be observed that RSO reaches the equilibrium in the first 10 min with a maximum removal percentage of 78. While for TSO the biosorption was proceeded in two steps. The first step is up to 10 min and is characterized by quick biosorption with a maximum removal percentage of 69. The second step is a slow biosorption to the final equilibrium at 40 min with a maximum removal percentage of 78. Therefore, it can be concluded that RSO reaches equilibrium

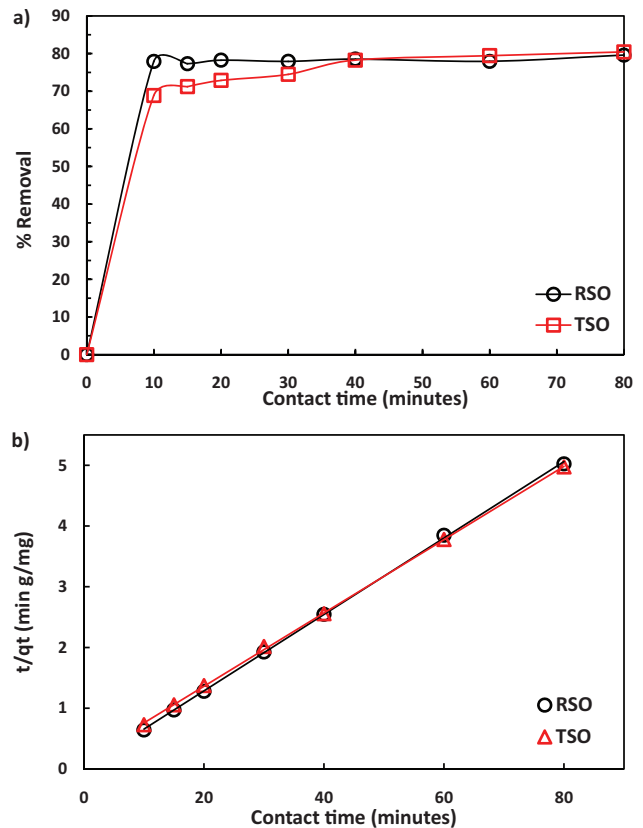


Fig. 4. (a) Effect of contact time on the removal of MB and (b) plots of pseudo-second-order kinetics. Experimental conditions: dose, 1 g/L; C_i 20 mg/L and pH, 6.5.

faster than the TSO and achieves higher removal percentage. Similar trend have been reported for the biosorption of MB on algal biomasses [18,20,21].

The biosorption kinetics was further analyzed by applying the linear forms of the pseudo-first-order (Eq. (3)) and pseudo-second-order models (Eq. (4)).

$$\log(q_e - q_t) = \log q_e - \frac{k_1 t}{2.303} \tag{3}$$

$$\frac{t}{q_t} = \frac{1}{k_2 q_e^2} + \frac{1}{q_e} t \quad (4)$$

where q_t (mg/g) is the amount of MB sorbed per gram of biomasses at time t (min), k_1 (1/min) and k_2 (g/mg min.) are the pseudo-first-order and pseudo-second-order rate constant, respectively.

Both pseudo-first-order and pseudo-second-order equations rely on the sorption capacity of the sorbent. However, the pseudo-first-order equation expects only the initial stage of the sorption process where rapid sorption occurs, while the pseudo-second-order equation expects the sorption behavior over the whole contact time range. Also, the pseudo-second-order model assumes that chemisorption controls the sorption rate [16,23].

Table 2 lists the kinetic parameters calculated from linear regression for the two models. The correlation coefficient (R^2) and the calculated q_e values clearly show that the pseudo-second-order model (Fig. 4(b)) describes the time profile for the biosorption process for both biomasses much better than the pseudo-first-order model.

Fitting to the pseudo-second-order kinetic model suggests that the chemical interactions between surface functional groups of biomasses and MB molecules control the rate of the biosorption process. Table 2 shows that the adsorption kinetics for RSO is six times that for TSO. Similar trend have been reported by previous studies [16,18,22].

3.4. Equilibrium studies and isotherm modeling

3.4.1. The distribution coefficient

The distribution coefficient between the biosorbent and aqueous phase, K_d , is the ratio of the amount of an adsorbate bounded to a biosorbent to the aqueous phase concentration at equilibrium [29,30]. To understand the distribution of MB between the studied biosorbents and aqueous phase, K_d (L/g) was calculated by Eq. (5):

$$K_d = \frac{q_e}{C_e} \quad (5)$$

Fig. 5 shows K_d as a function of initial MB concentrations. We can observe that (i) the K_d values for RSO were significantly

higher than those for TSO, and (ii) for RSO, the K_d values were almost constant up to $C_i = 60$ mg/L. But, further increment in the C_i results in a decrease in the K_d values. While for TSO, the K_d values decrease with increasing C_i up to 40 mg/L then hardly changed. These observations indicate that, RSO is a better biosorbent for MB than TSO, especially at high C_i . In addition, decreasing K_d with C_i might be due to the involvement of energetically less favorable sites with increasing C_i .

3.4.2. Langmuir isotherm

The Langmuir model assumes a homogeneous adsorbent surface that contains a fixed number of adsorption sites, and that the adsorbed molecules form a monolayer on the adsorbent surface and did not interact with each other [31]. The linear form of the Langmuir isotherm is shown by Eq. (6):

$$\frac{C_e}{q_e} = \frac{1}{Q_o K_L} + \frac{1}{Q_o} C_e \quad (6)$$

where Q_o is the maximal adsorption capacity, that is, the amount of MB adsorbed per gram of the biomass to form a complete monolayer on the surface (mg/g), while K_L is a constant related to the energy of interaction with the surface [32].

Although Fig. 6 illustrates a linear relationship of C_i/q_e vs. C_e using the experimental data obtained, the R^2 values indicate the poor fitting of Langmuir model to the biosorption data. Thus, the model could not be used to reliably extract further interpretation of the isotherm.

3.4.3. Freundlich isotherm

The Freundlich isotherm model assumes that the adsorption sites are heterogeneous and the adsorbed molecules interacts with each other [33]. The linearized form of Freundlich isotherm is presented by Eq. (7):

$$\log q_e = \log K_f + \frac{1}{n} \log C_e \quad (7)$$

where K_f is the Freundlich constant related to the adsorption capacity while n is a constant related to adsorption intensity; if $n = 1$, then adsorption is linear; if $n < 1$,

Table 2
Kinetics models driven parameters

| Model | Parameter | Biomass | |
|---------------------|-------------|---------|--------|
| | | RSO | TSO |
| Pseudo-first-order | $q_{e,exp}$ | 15.92 | 16.09 |
| | R^2 | 0.6091 | 0.9514 |
| | $q_{e,cal}$ | 1.78 | 6.84 |
| Pseudo-second-order | k_1 | 0.023 | 0.084 |
| | R^2 | 0.9998 | 0.9997 |
| | $q_{e,cal}$ | 15.90 | 16.56 |
| | k_2 | 0.144 | 0.024 |

Note: $q_{e,exp}$ and $q_{e,cal}$ are the amount of MB sorbed per gram of biomass at equilibrium obtained from experiment and calculated from the kinetic model, respectively.

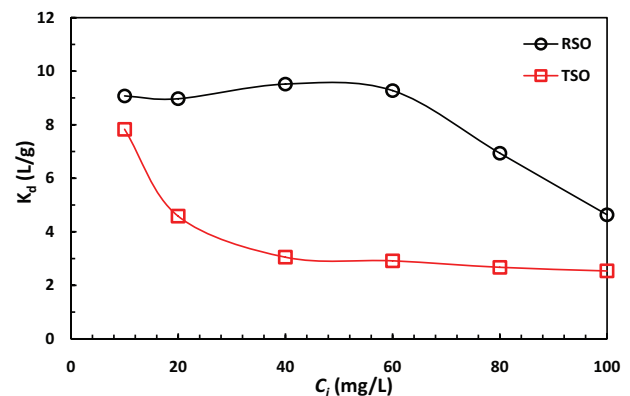


Fig. 5. Variation of K_d as a function of initial concentration. Experimental conditions: dose, 1.2 g/L; pH, 5 and contact time, 40 min.

then adsorption is a chemical process; if $n > 1$, then adsorption is a physical process [34].

The plot of $\log q_e$ vs. $\log C_e$ for the biosorption of MB onto the studied biomasses gives straight lines with R^2 values >0.9 (Fig. 7) indicating that biosorption follows the Freundlich isotherm. Consequently, Freundlich constants, K_f and $1/n$ were calculated and listed in Table 3.

K_f is an indicator of adsorption capacity; as the K_f value increases, the sorption capacity increases [35–39]. On the other hand, the magnitude of the exponent n gives indication on the affinity between sorbent and sorbate and the nature of sorption process. It is generally argued that the affinity between sorbent and sorbate increases when $1/n$ value decrease [26]. In addition, a $1/n$ value below unity implies chemisorption process [40]. Values of K_f shown in Table 2 indicate that RSO has the higher adsorption capacity than TSO. While $1/n$ values indicate that the sorption is a chemisorption process and TSO has higher affinity to MB.

3.4.4. Dubinin–Radushkevich isotherm

The D–R isotherm is very useful for predicting the mechanism and nature of biosorption process. It can be presented by Eq. (8):

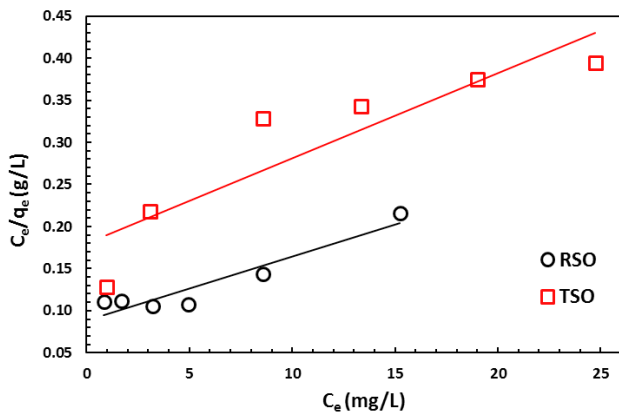


Fig. 6. Langmuir isotherm model for the MB biosorption onto RSO and TSO.

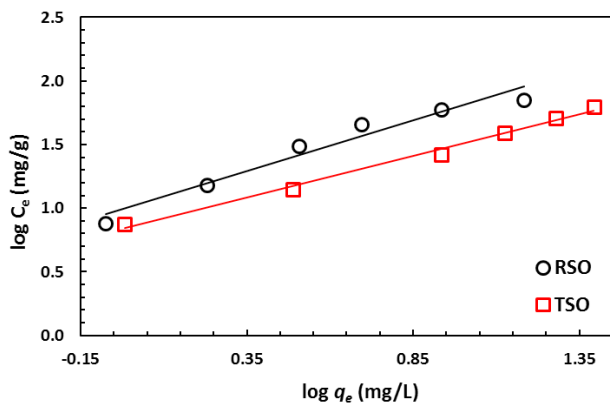


Fig. 7. Freundlich isotherm model for the MB biosorption onto RSO and TSO.

$$\ln q_e = \ln q_m - \beta \epsilon^2 \tag{8}$$

where q_m is D–R monolayer capacity (mg/g), β is parameter related to sorption energy E , defined as: $E = 1/\sqrt{-2\beta}$ and ϵ is Polanyi potential, defined as: $\epsilon = RT \ln(1 + 1/C_e)$ where R is the universal gas constant (8.314 J mol/K) and T is the absolute temperature (K).

The value of E gives information about the nature of the biosorption either it is a chemical or physical process. E value ranges from 1 to 8 kJ/mol indicates physical adsorption and from 8 to 16 kJ/mol indicates chemisorption.

The biosorption data were analyzed according to the linear form of the D–R isotherm and the linear plots are presented in Fig. 8. According to the values of R^2 (Table 3), the D–R isotherm fits the experimental data satisfactorily. Hence, the calculated E values (recoded in Table 2) indicate that chemisorption may play a significant role in the adsorption process. This result supports the suggestion given by the $1/n$ values derived from Freundlich model.

4. Conclusions

The performance of the raw and CaCl_2 treated biomass for the biosorption of water containing dyes was investigated by studying the factors affecting the sorption process in addition to modeling of the equilibrium data. The FTIR analysis of the biomasses verified the existence of

Table 3
Isotherm models driven parameters

| Model | Parameter | Biomass | |
|----------------------|--------------|---------|--------|
| | | RSO | TSO |
| Langmuir | R^2 | 0.8982 | 0.8179 |
| | Q_o | 131.6 | 99.0 |
| | K_L | 0.001 | 0.002 |
| Freundlich | R^2 | 0.9563 | 0.9917 |
| | K_f | 10.29 | 7.18 |
| | $1/n$ | 0.80 | 0.65 |
| Dubinin–Radushkevich | R^2 | 0.9699 | 0.9832 |
| | E (kJ/mol) | 9.35 | 10.23 |

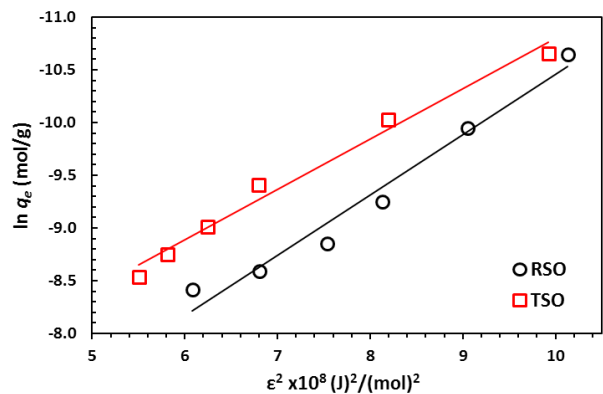


Fig. 8. D–R isotherm model for the MB biosorption onto RSO and TSO.

charged functional groups such as amino, carboxyl and hydroxyl in the biomass cell wall. The intensities of these groups decreased after the sorption of MB indicating their important role in the sorption process. The sorption results demonstrated that the contact time and biomass dosage have a great effect on the sorption process. The kinetics of MB biosorption was best described by pseudo-second-order kinetic model rather than pseudo-first-order. The $q_{e,cal}$ using pseudo-second-order kinetic model was very close to the $q_{e,exp}$. The equilibrium data were accurately described by Freundlich model. In addition, both Freundlich and Dubinin–Radushkevich models indicate that the MB uptake by the biomasses is a chemisorption process. Finally, it can be concluded that *S. obliquus* can efficiently remove MB from aqueous medium and the treatment of *S. obliquus* with $CaCl_2$ has detrimental effect on its sorption capacity.

References

- [1] Y. Bulut, H. Aydın, A kinetics and thermodynamics study of methylene blue adsorption on wheat shells, *Desalination*, 194 (2006) 259–267.
- [2] M. Auta, B. Hameed, Acid modified local clay beads as effective low-cost adsorbent for dynamic adsorption of methylene blue, *J. Ind. Eng. Chem.*, 19 (2013) 1153–1161.
- [3] A.N. Kabra, R.V. Khandare, S.P. Govindwar, Development of a bioreactor for remediation of textile effluent and dye mixture: a plant–bacterial synergistic strategy, *Water Res.*, 47 (2013) 1035–1048.
- [4] A.K. Verma, R.R. Dash, P. Bhunia, A review on chemical coagulation/flocculation technologies for removal of colour from textile wastewaters, *J. Environ. Manage.*, 93 (2012) 154–168.
- [5] J.-S. Bae, H.S. Freeman, Aquatic toxicity evaluation of new direct dyes to the *Daphnia magna*, *Dyes Pigm.*, 73 (2007) 81–85.
- [6] M. Oz, D.E. Lorke, G.A. Petroianu, Methylene blue and Alzheimer's disease, *Biochem. Pharmacol.*, 78 (2009) 927–932.
- [7] V. Vadivelan, K.V. Kumar, Equilibrium, kinetics, mechanism, and process design for the sorption of methylene blue onto rice husk, *J. Colloid Interface Sci.*, 286 (2005) 90–100.
- [8] D. Zhang, C. Ran, Y. Yang, Y. Ran, Biosorption of phenanthrene by pure algae and field-collected planktons and their fractions, *Chemosphere*, 93 (2013) 61–68.
- [9] T. Akar, A. Kulcu, S.T. Akar, Effective decolorization potential of *Thamnidium elegans*: biosorption optimization, modelling, characterization and application studies, *Chem. Eng. J.*, 221 (2013) 461–468.
- [10] M. Ghaedi, S. Hajati, B. Barazesh, F. Karimi, G. Ghezalbash, *Saccharomyces cerevisiae* for the biosorption of basic dyes from binary component systems and the high order derivative spectrophotometric method for simultaneous analysis of Brilliant green and Methylene blue, *J. Ind. Eng. Chem.*, 19 (2013) 227–233.
- [11] Y. Yang, G. Wang, B. Wang, Z. Li, X. Jia, Q. Zhou, Y. Zhao, Biosorption of Acid Black 172 and Congo Red from aqueous solution by nonviable *Penicillium* YW 01: kinetic study, equilibrium isotherm and artificial neural network modeling, *Bioresour. Technol.*, 102 (2011) 828–834.
- [12] A.M. Abdel-Aty, T.A. Gad-Allah, M.E. Ali, H.H. Abdel-Ghafar, Parametric, equilibrium, and kinetic studies on biosorption of diuron by *Anabaena sphaerica* and *Scenedesmus obliquus*, *Environ. Prog. Sustainable Energy*, 34 (2015) 504–511.
- [13] A. Khataee, F. Vafaei, M. Jannatkah, Biosorption of three textile dyes from contaminated water by filamentous green algal *Spirogyra* sp.: kinetic, isotherm and thermodynamic studies, *Int. Biodeterior. Biodegrad.*, 83 (2013) 33–40.
- [14] N.F. Cardoso, E.C. Lima, B. Royer, M.V. Bach, G.L. Dotto, L.A. Pinto, T. Calvete, Comparison of *Spirulina platensis* microalgae and commercial activated carbon as adsorbents for the removal of Reactive Red 120 dye from aqueous effluents, *J. Hazard. Mater.*, 241 (2012) 146–153.
- [15] M. Kousha, E. Daneshvar, H. Dopeikar, D. Taghavi, A. Bhatnagar, Box–Behnken design optimization of Acid Black 1 dye biosorption by different brown macroalgae, *Chem. Eng. J.*, 179 (2012) 158–168.
- [16] J. Vijayaraghavan, T. Bhagavathi Pushpa, S. Sardhar Basha, J. Jegan, Isotherm, kinetics and mechanistic studies of methylene blue biosorption onto red seaweed *Gracilaria corticata*, *Desal. Wat. Treat.*, 57 (2016) 13540–13548.
- [17] E. Rubin, P. Rodriguez, R. Herrero, M.E. Sastre de Vicente, Adsorption of methylene blue on chemically modified algal biomass: equilibrium, dynamic, and surface data, *J. Chem. Eng. Data*, 55 (2010) 5707–5714.
- [18] A. El Sikaily, A. Khaled, A.E. Nemr, O. Abdelwahab, Removal of methylene blue from aqueous solution by marine green alga *Ulva lactuca*, *Chem. Ecol.*, 22 (2006) 149–157.
- [19] V.J. Vilar, C.M. Botelho, R.A. Boaventura, Methylene blue adsorption by algal biomass based materials: biosorbents characterization and process behaviour, *J. Hazard. Mater.*, 147 (2007) 120–132.
- [20] M. Ncibi, A.B. Hamissa, A. Fathallah, M. Kortas, T. Baklouti, B. Mahjoub, M. Seffen, Biosorptive uptake of methylene blue using Mediterranean green alga *Enteromorpha* spp., *J. Hazard. Mater.*, 170 (2009) 1050–1055.
- [21] D. Caparkaya, L. Cavas, Biosorption of methylene blue by a brown alga *Cystoseira barbatula* Kützinger, *Acta Chim. Slov.*, 55 (2008) 547–553.
- [22] E. Daneshvar, A. Vazirzadeh, A. Niazi, M. Sillanpää, A. Bhatnagar, A comparative study of methylene blue biosorption using different modified brown, red and green macroalgae – effect of pretreatment, *Chem. Eng. J.*, 307 (2017) 435–446.
- [23] Z. Aksu, Application of biosorption for the removal of organic pollutants: a review, *Process Biochem.*, 40 (2005) 997–1026.
- [24] E. Daneshvar, M. Kousha, M.S. Sohrabi, B. Panahbehagh, A. Bhatnagar, H. Younesi, S.P.K. Sternberg, Application of response surface methodology for the biosorption of Acid Blue 25 dye using raw and HCl-treated macroalgae, *Desal. Wat. Treat.*, 53 (2015) 1710–1723.
- [25] W.W. Carmichael, Isolation, Culture, and Toxicity Testing of Toxic Freshwater Cyanobacteria (Blue-Green Algae), *Fundamental Research in Homogenous Catalysis*, Vol. 3, 1986, pp. 1249–1262.
- [26] H.H. Abdel Ghafar, A.M. Abdel-Aty, N.S. Ammar, M.A. Embaby, Lead biosorption from aqueous solution by raw and chemically modified green fresh water algae *Scenedesmus obliquus*, *Desal. Wat. Treat.*, 52 (2014) 7906–7914.
- [27] M. Ahmaruzzaman, Adsorption of phenolic compounds on low-cost adsorbents: a review, *Adv. Colloid Interface Sci.*, 143 (2008) 48–67.
- [28] M.C. Ncibi, B. Mahjoub, M. Seffen, Kinetic and equilibrium studies of methylene blue biosorption by *Posidonia oceanica* (L.) fibres, *J. Hazard. Mater.*, 139 (2007) 280–285.
- [29] E.N. El Qada, S.J. Allen, G.M. Walker, Adsorption of Methylene Blue onto activated carbon produced from steam activated bituminous coal: a study of equilibrium adsorption isotherm, *Chem. Eng. J.*, 124 (2006) 103–110.
- [30] Q.W. Chow, Predicting Adsorption Isotherms in Natural Water Using Polyparameter Linear Free Energy Relationships, University of Illinois at Urbana-Champaign, 2010.
- [31] I. Langmuir, The adsorption of gases on plane surfaces of glass, mica and platinum, *J. Am. Chem. Soc.*, 40 (1918) 1361–1403.
- [32] S. Marković, A. Stanković, Z. Lopičić, S. Lazarević, M. Stojanović, D. Uskoković, Application of raw peach shell particles for removal of methylene blue, *J. Environ. Chem. Eng.*, 3 (2015) 716–724.
- [33] H.M.F. Freundlich, Over the adsorption in solution, *J. Phys. Chem.*, 57 (1906) 385–470.
- [34] M.B. Desta, Batch sorption experiments: Langmuir and Freundlich isotherm studies for the adsorption of textile metal ions onto Teff Straw (*Eragrostis tef*) agricultural waste, *J. Thermodyn.*, 2013 (2013) 1–6.
- [35] S. Mukherjee, S. Kumar, A.K. Misra, M. Fan, Removal of phenols from water environment by activated carbon, bagasse ash and wood charcoal, *Chem. Eng. J.*, 129 (2007) 133–142.

- [36] B.H. Hameed, Equilibrium and kinetics studies of 2,4,6-trichlorophenol adsorption onto activated clay, *Colloids Surf., A*, 307 (2007) 45–52.
- [37] P. Girods, A. Dufour, V. Fierro, Y. Rogaume, C. Rogaume, A. Zoulalian, A. Celzard, Activated carbons prepared from wood particleboard wastes: characterisation and phenol adsorption capacities, *J. Hazard. Mater.*, 166 (2009) 491–501.
- [38] C. Solisio, A. Lodi, M.D. Borghi, Treatment of effluent containing micropollutants by means of activated carbon, *Waste Manage.*, 21 (2001) 33–40.
- [39] N. Tancredi, N. Medero, F. Möller, J. Píriz, C. Plada, T. Cordero, Phenol adsorption onto powdered and granular activated carbon, prepared from *Eucalyptus* wood, *J. Colloid Interface Sci.*, 279 (2004) 357–363.
- [40] K.Y. Foo, B.H. Hameed, Insights into the modeling of adsorption isotherm systems, *Chem. Eng. J.*, 156 (2010) 2–10.